The direct Method of Fundamental Solutions and the inverse Kirsch-Kress Method for the reconstruction of elastic inclusions or cavities

Carlos J. S. Alves[1], Nuno F. M. Martins[2]

[1] CEMAT-IST and Departamento de Matemática, Instituto Superior Técnico, TULisbon, Avenida Rovisco Pais, 1096 Lisboa Codex, Portugal (calves@math.ist.utl.pt)
[2] CEMAT-IST and Departamento de Matemática, Faculdade de Ciências e Tecnologia, Univ. Nova de Lisboa, Quinta da Torre, 2829-516 Caparica, Portugal (nfm@fct.unl.pt)

This paper is dedicated to Professor Rainer Kress on the occasion of his 65th birthday.

Abstract: In this work we consider the inverse problem of detecting inclusions or cavities in an elastic body, using a single boundary measurement on an external boundary. We discuss the identifiability questions on shape reconstruction, presenting counterexamples for Robin boundary conditions or with additional unknown Lamé parameters. Using the method of fundamental solutions (MFS) we adapt a method introduced twenty years ago by Andreas Kirsch and Rainer Kress [17] (in the context of an exterior problem in acoustic scattering) to this inverse problem in a bounded domain. We prove density results that justify the reconstruction of the solution from the Cauchy data using the MFS. We also establish some connections between this linear part of the Kirsch-Kress method and the direct MFS, through matrices of boundary layer integrals. Several numerical examples are presented, showing that with noisy data we were able to retrieve a fairly good reconstruction of the shape (or of its convex hull) with this MFS version of the Kirsch-Kress method.

1 Introduction

The identification of inclusions or cavities in an elastic body from external boundary measurements is a problem in nondestructive testing. This is an inverse problem that aims to reconstruct the shape and location of the burried object from the knowledge of the Cauchy data. This problem has been addressed in the literature for both scalar and vectorial potential problems with different boundary conditions. For the Laplace equation, with applications in thermal imaging see for instance [9], [15], [16] and more recently [10] where an unknown Robin boundary condition was considered. For the elasticity (or elastodynamic) system, see the review paper by M. Bonnet [8]. Some recent works considered the detection of small diameter inclusions (eg. [2], [4]) or spherical inclusions (eg. [6]). The detection of elastic cavities and inclusions can also be analysed in a different framework in terms of a change in the elastic material properties (e.g. [1], [21], [23]).

In this work, we address the aforementioned inverse problem considering a single boundary measurement on an accessible part of the external boundary. The buried object is either a rigid inclusion (defined by a Dirichlet boundary condition), a cavity (defined by a Neumann like boundary condition) or a more general inclusion (defined by a Robin like boundary condition). The identifiability questions are discussed in Section 2 and in Section 3 we focus on the numerical resolution of the inverse problem.

We propose a numerical scheme that connects the Method of Fundamental Solutions (MFS), proposed forty years ago by Kupradze and Aleksidze [18], and the Kirsch-Kress Method (KKM), proposed twenty years ago [17]. The MFS was usually presented as a numerical method for direct problems, but it has gained recently some popularity as a method to solve some Cauchy problems (eg. [20]). This feature was already present in the original formulation of the Kirsch-Kress Method (for acoustic scattering) using single layer potentials, that consists in two parts: (i) linear part - resolution of the Cauchy problem, (ii) nonlinear part - recovering the level set by an optimization technique. This connection is here made clear by analysing the operator matrices with boundary potentials for both the MFS and the KKM. Although density results are deduced for both methods, these share an ill-conditioned feature that can be dealt with a Tikhonov regularization technique.

In Section 4 several numerical examples show the possibilities (and some difficulties) of the MFS used in the KKM sense, for these elastic inverse problems, considering unknown rigid inclusions. This technique was previously tested for scalar (Laplace) problems with better reconstruction results[1], which can be explained by the difficulties in obtaining a level curve in the vectorial case. Nevertheless this proved to be a quite fast numerical scheme that enables a good approximation of the location and shape of the unknown inclusion even with considerable noisy data.

2 Direct and Inverse Problem

We consider an isotropic and homogeneous elastic body $\Omega \subset \mathbb{R}^d$ with inclusions or cavities represented by ω. We assume that Ω is an open bounded simply connected set and ω is open, bounded and the disjoint union of simply connected sets, with regular (C^1) boundaries $\Gamma = \partial\Omega$ and $\gamma = \partial\omega$ such that $\overline{\omega} \subset \Omega$. We define the domain of elastic propagation by

$$\Omega_c := \Omega \setminus \overline{\omega}$$

and note that $\partial\Omega_c = \Gamma \cup \gamma$.

In linearized elasticity, using Hooke's law, the stress tensor σ is defined in terms of the displacement vector $\mathbf{u}$ by

$$\sigma_{\lambda,\mu}(\mathbf{u}) = \lambda(\nabla \cdot \mathbf{u})\mathbf{I} + \mu\left(\nabla\mathbf{u} + \nabla\mathbf{u}^\top\right)$$

where λ and μ are the *Lamé coefficients*. When there is no body force and the body is in static equilibrium, the equations of motion resume to a null divergence of the stress, giving the Lamé system of equations

$$\nabla \cdot \sigma_{\lambda,\mu}(\mathbf{u}) = \mathbf{0}.$$

We will write $\Delta^*_{\lambda,\mu}\mathbf{u} := \nabla \cdot (\sigma_{\lambda,\mu}(\mathbf{u}))$, noticing that

$$\nabla \cdot \sigma_{\lambda,\mu}(\mathbf{u}) = \mu\Delta\mathbf{u} + (\lambda+\mu)\nabla\nabla \cdot \mathbf{u},$$

and we will use the notation $\partial^*_{\lambda,\mu}\mathbf{u} := \sigma_{\lambda,\mu}(\mathbf{u})\mathbf{n}$ for the surface traction vector, where $\mathbf{n}$ is the outward normal vector.

- *Direct problem:* Given $\mathbf{g} \in H^{1/2}(\Gamma)^d$, determine $\partial^*_{\lambda,\mu}\mathbf{u}$ on Γ, such that $\mathbf{u}$ that satisfies

$$(\mathcal{P}_{\Omega_c}) \quad \begin{cases} \Delta^*_{\lambda,\mu}\mathbf{u} = \mathbf{0} & \text{in } \Omega_c \\ \mathbf{u} = \mathbf{g} & \text{on } \partial\Omega = \Gamma \\ \mathcal{B}\mathbf{u} = \mathbf{0} & \text{on } \partial\omega = \gamma \end{cases}$$

[1] Communication by the authors in the International Workshop on Integral Equations and Shape Reconstruction (Göttingen, Germany, 2007).

with known Lamé coefficients $\lambda, \mu > 0$. Here $\mathcal{B}$ stands for one of the classic boundary trace operators: $\mathcal{B}\mathbf{u} = \mathbf{u}$ (Dirichlet, ω is a rigid inclusion) or $\mathcal{B}\mathbf{u} = \partial^*_{\lambda,\mu}\mathbf{u}$ (Neumann, ω is a cavity) or $\mathcal{B}\mathbf{u} = \partial^*_{\lambda,\mu}\mathbf{u} + \mathbf{Z}\mathbf{u}$ (Robin, ω is an inclusion). This direct problem is well posed with solution $\mathbf{u} \in H^1(\Omega_c)^d$ (for the Robin condition, consider also $\mathbf{Z}$ to be a $L^\infty(\gamma)$ positive definite matrix function).

- *Inverse problem:* From the known input displacement $\mathbf{g}$ and the measured surface traction $\partial^*_{\lambda,\mu}\mathbf{u}$ on a part Σ of the external boundary, ie. $\Sigma \subseteq \Gamma = \partial\Omega$, we aim to identify the shape of the internal boundary $\gamma = \partial\omega$ (and therefore the inclusion or the cavity ω).

It is well known that the recovery of a solution from Cauchy data is an ill posed problem in the Hadamard sense. In terms of the inverse problem, this means (assuming uniqueness of the inverse problem) noise sensitive reconstructions. The uniqueness of the inverse problem is addressed in the next section.

Remark 1. *The direct problems will also be addressed in a more general formulation*

$$(\widetilde{\mathcal{P}}_{\Omega_c}) \quad \left\{ \begin{array}{ll} \Delta^*_{\lambda,\mu}\mathbf{u} = \mathbf{0} & \text{in } \Omega_c \\ \widetilde{\mathcal{B}}\mathbf{u} = \widetilde{\mathbf{g}} & \text{on } \partial\Omega_c \end{array} \right. \tag{1}$$

where $\widetilde{\mathcal{B}}$ is the boundary operator defined by

$$\widetilde{\mathcal{B}}\mathbf{u} = a\ \partial^*_{\lambda,\mu}\mathbf{u} + \widetilde{\mathbf{Z}}_a\mathbf{u} \tag{2}$$

with $\widetilde{\mathbf{g}}|_\gamma = 0$, $a \in \{0,1\}$ constant on γ and $\widetilde{\mathbf{Z}}_0 = \mathbf{I}$. In this case, a compatibility condition would be required for the pure Neumann problem. Although we focus in the framework $(\mathcal{P}_{\Omega_c})$, it is clear that some of the following results could be easily obtained in the more general formulation $(\widetilde{\mathcal{P}}_{\Omega_c})$.

2.1 Identifiability

2.1.1 Non-identifiability cases (single measurement):

(i) *Robin boundary condition.*
As shown by Cakoni and Kress in [10], for the Laplace equation, a single boundary measurement may not suffice to identify an inclusion ω with Robin boundary conditions. This non identification also occurs in the elastic case. For instance, consider the function defined in $\mathbb{R}^2 \setminus \{\mathbf{0}\}$ by

$$\mathbf{u}(\mathbf{x}) = \mathbf{x} - \nabla \log |\mathbf{x}| \tag{3}$$

and the annular domain $\Omega_c = \Omega \setminus \overline{\omega}$ where $\Omega = B(\mathbf{0},\mathrm{P}) = \left\{\mathbf{x} \in \mathbb{R}^2 : |\mathbf{x}| < \mathrm{P}\right\}$, $\omega = B(\mathbf{0},\rho)$ and $0 < \rho < \mathrm{P}$. A forward computation gives, on $\gamma = \partial\omega$

$$\partial^*_{\lambda,\mu}\mathbf{u}|_\gamma = \frac{2+4\rho^2}{\rho^2}\mathbf{n} \ \wedge\ \mathbf{u}|_\gamma = -\frac{1-\rho^2}{\rho}\mathbf{n}.$$

Since $\mathbf{u}$ solves the Lamé system in $\mathbb{R}^2 \setminus \{\mathbf{0}\}$, we have

$$\left\{ \begin{array}{ll} \Delta^*_{\lambda,\mu}\mathbf{u} = 0 & \text{in } \Omega_c \\ \mathbf{u} = \mathbf{g} & \text{on } \Gamma \\ \partial^*_{\lambda,\mu}\mathbf{u} + \mathbf{Z}_\rho\mathbf{u} = \mathbf{0} & \text{on } \gamma \end{array} \right.$$

where $\mathbf{g}$ is the restriction of $\mathbf{u}$ to $\Gamma = \partial\Omega$ and

$$\mathbf{Z}_\rho = \frac{2+4\rho^2}{\rho(1-\rho^2)}\mathbf{I}.$$

Since the function $\rho \to \frac{2+4\rho^2}{\rho(1-\rho^2)}$ is not injective for $0 < \rho < 1$ (... it has a derivative zero in $\rho = \frac{1}{2}\sqrt{-5+\sqrt{33}} \approx 0.43$) then at least two circular inclusions generate the same Cauchy data on Γ.

(ii) *Unknown Lamé coefficients.*
In [23], Nakamura and Uhlmann obtained, in a more general framework, a sufficient condition for the identification of Lamé coefficients, assuming the knowledge of the Dirichlet to Neumann map. A further analysis of the previous example shows that one measurement may not suffice for the identification of these constants. For instance, if $\rho = 1 < \mathrm{P}$, then $\mathbf{u}$ defined in (3) is the solution of the Dirichlet problem

$$\begin{cases} \Delta^*_{\lambda_0,\mu_0}\mathbf{u} = 0 & \text{in } \Omega_c \\ \mathbf{u} = \mathbf{g} & \text{on } \Gamma \\ \mathbf{u} = \mathbf{0} & \text{on } \gamma \end{cases}$$

with unknown Lamé constants λ_0 and μ_0. The Neumann data on Γ is

$$\partial^*_{\lambda_0,\mu_0}\mathbf{u}|_\Gamma = \frac{2(\mu_0 + \mathrm{P}^2(\lambda_0+\mu_0))}{\mathrm{P}^2}\mathbf{n}$$

therefore, the (non empty) set of Lamé constants

$$\left\{(\lambda,\mu) \in \mathbb{R}^2_+ : \mu - \mu_0 = \frac{\mathrm{P}^2}{1+\mathrm{P}^2}(\lambda_0 - \lambda)\right\}$$

generates the same data on the boundary, and identification is not possible.

2.1.2 Identifiability results

We now address the identification of inclusions or cavities defined by homogeneous Dirichlet or Neumann conditions. We start with a proof that extends to the elastic case the Holmgren lemma and analytic continuation arguments.

Lemma 2. *Let $\Omega \subset \mathbb{R}^d$ with C^1 boundary $\Gamma = \partial\Omega$ and consider $\Sigma \subset \Gamma$ open in the topology of Γ. If $\mathbf{f} \in \mathcal{E}'(\Omega)$, a compactly supported distribution, with support $\overline{\Omega}_\mathbf{f} \subset \Omega$ and $\Delta^*_{\lambda,\mu}\mathbf{u} = \mathbf{f}$ in Ω with null Cauchy data on Σ then $\mathbf{u} = \mathbf{0}$ in Ω_Σ, where Ω_Σ is the connected component of $\Omega \setminus \overline{\Omega}_\mathbf{f}$ such that $\Sigma \subset \partial\Omega_\Sigma$.*

Proof. Consider the extension $\widetilde{\mathbf{u}}$ of $\mathbf{u}$ to the whole space by taking $\widetilde{\mathbf{u}} = 0$ in $\mathbb{R}^d \setminus \overline{\Omega}$. This extension can be given in convolution form by the boundary layers (e.g. [25] for the notation)

$$\widetilde{\mathbf{u}} = \mathbf{\Phi} * \mathbf{f} - \mathbf{\Phi} * [\partial^*_{\lambda,\mu}\mathbf{u}]\delta_\Gamma + \partial^*_{\lambda,\mu}(\mathbf{\Phi} * [\mathbf{u}]\delta_\Gamma) \tag{4}$$

where δ_Γ denotes the surface delta-characteristic distribution and $[\cdot]$ denotes the boundary jump. By hypothesis, both interior and exterior traces on Σ are null and $[\partial^*_{\lambda,\mu}\mathbf{u}]|_\Sigma = [\mathbf{u}]|_\Sigma = \mathbf{0}$, therefore

$$\widetilde{\mathbf{u}} = \mathbf{\Phi} * \mathbf{f} - \mathbf{\Phi} * [\partial^*_{\lambda,\mu}\mathbf{u}]\delta_{\Gamma\setminus\Sigma} + \partial^*_{\lambda,\mu}(\mathbf{\Phi} * [\mathbf{u}]\delta_{\Gamma\setminus\Sigma}).$$

Since the fundamental solution $\mathbf{\Phi}$ is analytic in $\mathbb{R}^d \setminus \{\mathbf{0}\}$ then this representation implies that $\widetilde{\mathbf{u}}$ is analytic in $\mathbb{R}^d \setminus (\overline{\Omega}_\mathbf{f} \cup (\Gamma \setminus \Sigma))$. On the other hand, $\widetilde{\mathbf{u}} = \mathbf{0}$ in $\mathbb{R}^d \setminus \overline{\Omega}$ hence, by analytic continuation through Σ, the solution $\mathbf{u}$ is null in those connected components. □

Remark 3. *The previous Lemma includes the case of distribuitions* $\mathbf{f}$ *that arise from the representation of boundary problems on the cavities* ω*, in terms of* $\mathbf{f} = \alpha\delta_\gamma + \partial^*_{\lambda,\mu}(\beta\delta_\gamma)$.
This proof can be extended to other linear elliptic differential operators with constant coefficients, where the fundamental solution exists (Malgrange-Ehrenpreis theorem) and is analytic in $\mathbb{R}^d \setminus \{\mathbf{0}\}$*, using the integral representation formulation.*

Theorem 4. *Assume that the boundary condition on the inclusion or cavity* γ *is defined by an homogeneous Dirichlet or Neumann condition. If* $\Sigma \subset \Gamma$ *is an open set in the topology of* Γ *and* $\mathbf{g}$ *is not constant, the Cauchy data on* Σ *determines uniquely* γ.

Proof. Suppose that Ω_c^1 and Ω_c^2 are different non-disjoint propagation domains with boundaries

$$\partial\Omega_c^1 = \Gamma \cup \gamma_1,\ \partial\Omega_c^2 = \Gamma \cup \gamma_2,$$

where γ_j refer to the boundary of the inclusion/cavity ω_j. Each ω_j $(j = 1, 2)$ can be the disjoint union of several simply connected components $\omega_j = \cup\omega_{j,k}$ and therefore $\gamma_j = \cup\gamma_{j,k}$.

Denote by $\mathbf{u}_1$ and $\mathbf{u}_2$ the solutions of problems $(\mathcal{P}_{\Omega_c^1})$ and $(\mathcal{P}_{\Omega_c^2})$ respectively. We show that, if

$$\mathbf{u}_1|_\Sigma = \mathbf{u}_2|_\Sigma,\ \partial^*_{\lambda,\mu}\mathbf{u}_1|_\Sigma = \partial^*_{\lambda,\mu}\mathbf{u}_2|_\Sigma$$

then $\mathbf{u}_1$ is constant in $\Omega_c^\#$, where $\Omega_c^\#$ denotes the connected component of $\Omega_c^1 \cap \Omega_c^2$ that contains Γ.
By the previous Lemma, the same Cauchy data on Σ implies

$$\mathbf{u}_1 = \mathbf{u}_2 \text{ in } \Omega_c^\#.$$

Now, $\partial\Omega_c^\# = \Gamma \cup \gamma_1^\# \cup \gamma_2^\#$ with $\gamma_j^\# \subset \gamma_j$ and $\gamma_1^\# \cap \gamma_2^\# = \emptyset$. Without loss of generality assume that $\gamma_2^\#$ is not empty and let $\omega_{2,k}$ be a simply connected component such that $\gamma_2^\# \cap \gamma_{2,k}$ is not empty.

If $\Omega_c^1 \cap \Omega_c^2$ is connected, ie $\Omega_c^1 \cap \Omega_c^2 = \Omega_c^\#$, then take $\sigma = \omega_{2,k} \setminus \overline{\omega}_1 \subset \Omega_c^1$ which is an open set with boundary $\partial\sigma \subset \gamma_2^\# \cup \gamma_1$. It is clear that $\Delta^*_{\lambda,\mu}\mathbf{u}_1 = 0$ in σ and on γ_1 we have null Dirichlet/Neumann data. By the previous Lemma, $\mathbf{u}_1$ has also null Dirichlet/Neumann data on $\gamma_2^\#$.

If $\Omega_c^1 \cap \Omega_c^2$ is not connected, take σ as the connected component of $\Omega_c^1 \setminus \overline{\Omega_c^\#}$ that intersects $\omega_{2,k}$. Again, $\partial\sigma \subset \gamma_2^\# \cup \gamma_1$ and in both cases we have

$$\begin{cases} \Delta^*_{\lambda,\mu}\mathbf{u}_1 = 0 & \text{in } \sigma \\ \mathcal{B}\mathbf{u}_1 = 0 & \text{in } \partial\sigma \end{cases} \tag{5}$$

where $\mathcal{B}$ is the trace or the normal trace operator. Thus, $\mathbf{u_1}$ is constant on σ (null, for the Dirichlet boundary condition) and we conclude, by analytic continuation, that $\mathbf{u_1}$ is constant in $\Omega_c^\#$. This contradicts the hypothesis because we have $\mathbf{g} = \mathbf{u}_1|_\Gamma$ is constant. □

Remark 5. *As shown in the non-identifiability counter-examples, the previous result can not be extended to the Robin problem. In the interior boundary problem (5)* $\mathcal{B}$ *could be defined by piecewise Robin coefficients* $\mathbf{Z}_j$ *(positive definite matrices) but the normal direction in* $\partial^*_{\lambda,\mu}$ *would have opposite sign on* γ_1.

3 MFS and KKM

3.1 The MFS in a multiconnected domain

Suppose that $\Omega_c \subset \mathbb{R}^d$ ($d = 2, 3$) is bounded, open and multiconnected. The complementary set $\mathbb{R}^d \setminus \overline{\Omega_c}$ has several connected components, one exterior $\Omega^{\mathrm{C}} = \mathbb{R}^d \setminus \bar{\Omega}$ and N interior connected components

(inclusions or cavities), $\omega_1, \ldots, \omega_N \subset \Omega$ with boundaries $\gamma_i = \partial\omega_i$. Again, we will denote ω the union of the components ω_i and γ is $\partial\omega$, the union of their boundaries.

To apply the Method of Fundamental Solutions, we will consider artificial sets that will define the location of the point-sources. These admissible sets are $\widehat{\gamma}_i = \partial\widehat{\omega}_i$ internal regular boundaries of $\widehat{\omega}_i$ simply connected open sets such that $\overline{\widehat{\omega}_i} \subset \omega_i$. Again, we will denote $\widehat{\omega}$ the union of the components $\widehat{\omega}_i$ and γ is $\partial\widehat{\omega}$ the union of the artificial inner boundaries. Finally, we define an external boundary $\widehat{\Gamma} = \partial\widehat{\Omega}$ with $\widehat{\Omega}$ an open unbounded set $\overline{\widehat{\Omega}} \subset \Omega^{\mathrm{C}}$ with a boundary that encloses the domain, $\Omega \subset \mathbb{R}^d \setminus \widehat{\Omega}$ (see Fig. 1). (The case with a bounded $\widehat{\Omega}$ is also possible, and theoretically simpler, but it gives worst numerical results when $\widehat{\Gamma}$ does not enclose the domain Ω.)

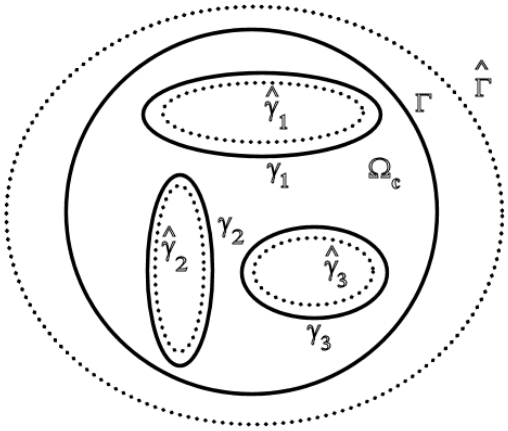

Figure 1: A multiconnected domain Ω_c with an artificial boundary $\widehat{\Gamma} \cup \widehat{\gamma}_1 \cup \widehat{\gamma}_2 \cup \widehat{\gamma}_3$.

Recall that the fundamental solution for the Lamé system is given by the tensor

$$[\mathbf{\Phi}(\mathbf{x})]_{ij} = \begin{cases} \frac{\lambda+3\mu}{4\pi\mu(\lambda+2\mu)} \left[-\log|\mathbf{x}|\delta_{ij} + \frac{\lambda+\mu}{\lambda+3\mu} \frac{x_i x_j}{|\mathbf{x}|^2} \right] & \text{2D case} \\ \frac{\lambda+3\mu}{8\pi\mu(\lambda+2\mu)} \left[\frac{1}{|\mathbf{x}|}\delta_{ij} + \frac{\lambda+\mu}{\lambda+3\mu} \frac{x_i x_j}{|\mathbf{x}|^3} \right] & \text{3D case} \end{cases}$$

and define the source tensor $\mathbf{\Phi}_y(x) := \mathbf{\Phi}(x-y)$.

Consider the single and double layer potential given in the integral form on a boundary S,

$$\mathbf{L}_S(\phi)(x) = \int_S \mathbf{\Phi}_x(y)\phi(y)dS_y, \ x \in \mathbb{R}^d \setminus S$$
$$\mathbf{M}_S\psi(x) = \int_S \partial^*_{\lambda,\mu}\mathbf{\Phi}_x(y)\psi(y)dS_y, \ x \in \mathbb{R}^d \setminus S$$

with $\phi \in H^{-1/2}(S)^d, \psi \in H^{1/2}(S)^d$. The boundary operator $\widetilde{\mathcal{B}} = a\tau^{\mathbf{n}}_{\Gamma\cup\gamma} + \mathbf{Z}_a\tau_{\Gamma\cup\gamma}$ is defined by the trace τ and normal trace $\tau^{\mathbf{n}} = \partial^*_{\lambda,\mu}$ on $\Gamma \cup \gamma$ as in (2).

Theorem 6. *The set* $\mathcal{S} = span\left\{\widetilde{\mathcal{B}}\mathbf{\Phi}_y : y \in \widehat{\gamma}\right\}$ *is dense in* $H^{1/2}(\Gamma\cup\gamma)^2/\mathbb{R}^2$ *(or* $H^{1/2}(\Gamma\cup\gamma)^3$ *in 3D).*

Proof. We prove that $\mathrm{Ker}((\widetilde{\mathcal{B}}\mathbf{L}_{\widehat{\Gamma}\cup\widehat{\gamma}})^*)$ is null, and this implies the density of the range of $\widetilde{\mathcal{B}}\mathbf{L}_{\widehat{\Gamma}\cup\widehat{\gamma}}$. Discretizing the smooth single layer potentials the density of the linear span $\mathcal{S}$ follows.

In 2D we consider

$$\mathcal{H}_{\mathbf{Z}}(\Gamma\cup\gamma)=\left\{\phi\in H^{1/2}(\Gamma\cup\gamma)^2:\int_{\Gamma\cup\gamma}\widetilde{\mathbf{Z}}_a(x)\phi(x)dS_x=0\right\},$$

which can be identified to $H^{1/2}(\Gamma\cup\gamma)^2/\mathbb{R}^p$ by taking a representative $\phi+\mathbf{C}$, defined by

$$\left(\int_{\Gamma\cup\gamma}\widetilde{\mathbf{Z}}_a\right)\mathbf{C}=\int_{\Gamma\cup\gamma}\widetilde{\mathbf{Z}}_a\phi,$$

being p the codimension of the matrix $\int_{\Gamma\cup\gamma}\widetilde{\mathbf{Z}}_a$.

First, we note that $(\widetilde{\mathcal{B}}\mathbf{L}_{\widehat{\Gamma}\cup\widehat{\gamma}})^*=\tau_{\widehat{\Gamma}\cup\widehat{\gamma}}(a\mathbf{M}_{\Gamma\cup\gamma}+\tau_{\widehat{\Gamma}\cup\widehat{\gamma}}\mathbf{L}_{\Gamma\cup\gamma}\mathbf{Z}_a)$, because

$$\begin{aligned}\left\langle\widetilde{\mathcal{B}}\mathbf{L}_{\widehat{\Gamma}\cup\widehat{\gamma}}\phi,\psi\right\rangle_{\Gamma\cup\gamma}&=\left\langle(a\tau^{\mathbf{n}}_{\Gamma\cup\gamma}\mathbf{L}_{\widehat{\Gamma}\cup\widehat{\gamma}}+\mathbf{Z}_a\tau_{\Gamma\cup\gamma}\mathbf{L}_{\widehat{\Gamma}\cup\widehat{\gamma}})\phi,\psi\right\rangle_{\Gamma\cup\gamma}\\&=\int_{\Gamma\cup\gamma}\left(a\partial^*_{\lambda,\mu}+\mathbf{Z}_a(x)\right)\int_{\widehat{\Gamma}\cup\widehat{\gamma}}\mathbf{\Phi}_y(x)\phi(y)dS_y\psi(x)dS_x\\&=\int_{\widehat{\Gamma}\cup\widehat{\gamma}}\int_{\Gamma\cup\gamma}\left(a\partial^*_{\lambda,\mu}+\mathbf{Z}_a(x)\right)\mathbf{\Phi}_y(x)\psi(x)dS_x\phi(y)dS_y\\&=\left\langle a\mathbf{M}_{\Gamma\cup\gamma}\psi+\mathbf{L}_{\Gamma\cup\gamma}\mathbf{Z}_a\psi,\phi\right\rangle_{\widehat{\Gamma}\cup\widehat{\gamma}}.\end{aligned}$$

Now, let $\psi\in\mathcal{H}_{\mathbf{Z}}(\Gamma\cup\gamma)$ (2D case) or $\psi\in H^{1/2}(\Gamma\cup\gamma)^3$ (3D case) and define the analytic function

$$\mathbf{u}(y)=(a\mathbf{M}_{\Gamma\cup\gamma}\psi+\mathbf{L}_{\Gamma\cup\gamma}\mathbf{Z}_a\psi)(y),\quad(y\in\mathbb{R}^d\setminus(\Gamma\cup\gamma)).$$

then $(\widetilde{\mathcal{B}}\mathbf{L}_{\widehat{\Gamma}\cup\widehat{\gamma}})^*\psi=\mathbf{0}$ is equivalent to $\mathbf{u}\equiv\mathbf{0}$ on $\widehat{\Gamma}\cup\widehat{\gamma}$. On the other hand, $\mathbf{u}$ verifies the Lamé system outside $\Gamma\cup\gamma$.

– Thus, $\mathbf{u}$ is the solution of the well posed exterior problem (cf. [11])

$$\left\{\begin{array}{lll}\Delta^*_{\lambda,\mu}\mathbf{u}=\mathbf{0}&&\text{in }\widehat{\Omega}\\\mathbf{u}=\mathbf{0}&&\text{on }\widehat{\Gamma}\\\mathbf{u}(y)=\left\{\begin{array}{ll}\log|y|\ \mathbf{a}_{\widetilde{\mathbf{Z}}}+\mathcal{O}(1)&\text{if }d=2\\\mathcal{O}(|y|^{-1})&\text{if }d=3\end{array}\right.&&|y|\to\infty\end{array}\right.$$

and uniqueness implies $\mathbf{u}=\mathbf{0}$ in $\widehat{\Omega}$. In the 2D case, the uniqueness follows by taking the asymptotic behavior with constant

$$\mathbf{a}_{\widetilde{\mathbf{Z}}}=\frac{\lambda+3\mu}{4\pi\mu(\lambda+2\mu)}\int_{\Gamma\cup\gamma}\widetilde{\mathbf{Z}}_a(x)\phi(x)dS_x,$$

hence $\mathbf{a}_{\widetilde{\mathbf{Z}}}=\mathbf{0}$ because $\phi\in\mathcal{H}_{\mathbf{Z}}(\Gamma\cup\gamma)$. In 3D the asymptotic behavior is immediately verified by the fundamental solution.

By analytic continuation $\mathbf{u}=0$ in $\widehat{\Omega}$ implies $\mathbf{u}$ null in Ω^{C} and the exterior traces $\mathbf{u}|^+_\Gamma$, $\partial^*_{\lambda,\mu}\mathbf{u}|^+_\Gamma$ are null. On the other hand, since

$$\mathbf{u}(y)=\int_{\Gamma\cup\gamma}a\ \partial^*_{\lambda,\mu}\mathbf{\Phi}_y(x)\phi(x)dS_x+\int_{\Gamma\cup\gamma}\widetilde{\mathbf{Z}}_a(x)\mathbf{\Phi}_y(x)\phi(x)dS_x$$

the boundary jumps on Γ are given by $[\mathbf{u}]_\Gamma=-a\ \phi|_\Gamma\ \wedge\ [\partial^*_{\lambda,\mu}\mathbf{u}]_\Gamma=\widetilde{\mathbf{Z}}_a\phi|_\Gamma$ and we conclude that

$$\mathbf{u}|^-_\Gamma=-a\ \phi|_\Gamma\ \wedge\ \partial^*_{\lambda,\mu}\mathbf{u}|^-_\Gamma=\widetilde{\mathbf{Z}}_a\phi|_\Gamma\ .$$

– Also, $\mathbf{u}$ is the solution of the well posed interior problems for each $j = 1, \ldots, N$,

$$\left\{ \begin{array}{ll} \Delta^*_{\lambda,\mu}\mathbf{u} = \mathbf{0} & \text{in } \widehat{\omega}_j \\ \mathbf{u} = \mathbf{0} & \text{on } \widehat{\gamma}_j \end{array} \right.$$

hence, $\mathbf{u} = \mathbf{0}$ in $\widehat{\omega}_j$. Again, by analytic continuation this implies $\mathbf{u} = \mathbf{0}$ in each ω_j and the exterior traces $\mathbf{u}|^+_{\gamma_j}$, $\partial^*_{\lambda,\mu}\mathbf{u}|^+_{\gamma_j}$ are null, thus

$$\mathbf{u}|^-_{\gamma_j} = -a\ \phi|_{\gamma_j}\ \wedge\ \partial^*_{\lambda,\mu}\mathbf{u}|^-_{\gamma_j} = \widetilde{\mathbf{Z}}_a\ \phi|^-_{\gamma_j}\ \text{ on }\ \gamma_j.$$

Therefore, $\mathbf{u}$ is also a solution of the interior problem

$$\left\{ \begin{array}{ll} \Delta^*_{\lambda,\mu}\mathbf{u}^- = \mathbf{0} & \text{in } \Omega_c \\ a\ \partial^*_{\lambda,\mu}\mathbf{u}^- + \widetilde{\mathbf{Z}}_a\mathbf{u}^- = \mathbf{0} & \text{on } \partial\Omega_c = \Gamma \cup \gamma \end{array} \right.$$

and by the well posedness of this problem we have $\mathbf{u}^- = \mathbf{0}$ in Ω_c. This implies that all traces $\mathbf{u}|^-_{\Gamma\cup\gamma}$ and $\partial^*_{\lambda,\mu}\mathbf{u}|^-_{\Gamma\cup\gamma}$ are null and, on the whole $\Gamma \cup \gamma$,

$$a\ \phi = [\mathbf{u}] = \mathbf{0} \wedge \widetilde{\mathbf{Z}}_a\phi = [\partial^*_{\lambda,\mu}\mathbf{u}] = \mathbf{0}$$

this implies $\phi = \mathbf{0}$, from the restrictions on $a, \widetilde{\mathbf{Z}}_a$. □

We now address the question of solving the direct problem $(\mathcal{P}_{\Omega_c})$ with the MFS.
Consider the solution of $(\widetilde{\mathcal{P}}_{\Omega_c})$ represented by the single layer potential that we separate into a sum

$$\mathbf{u} = \mathbf{L}_{\widehat{\Gamma}\cup\widehat{\gamma}}\psi = \mathbf{L}_{\widehat{\Gamma}}\psi|_{\widehat{\Gamma}} + \mathbf{L}_{\widehat{\gamma}}\psi|_{\widehat{\gamma}}. \tag{6}$$

On the boundary $\Gamma \cup \gamma$ we also separate the integral equations

$$\widetilde{\mathcal{B}}_\Gamma\mathbf{L}_{\widehat{\Gamma}\cup\widehat{\gamma}}\psi = \mathbf{g}, \quad \widetilde{\mathcal{B}}_\gamma\mathbf{L}_{\widehat{\Gamma}\cup\widehat{\gamma}}\psi = \mathbf{0} \tag{7}$$

with $\mathbf{g} \in H^{1/2}(\Gamma)^d$. This leads to a matrix operator system

$$\underbrace{\left[\begin{array}{cc} \widetilde{\mathcal{B}}_\Gamma\mathbf{L}_{\widehat{\Gamma}} & \widetilde{\mathcal{B}}_\Gamma\mathbf{L}_{\widehat{\gamma}} \\ \widetilde{\mathcal{B}}_\gamma\mathbf{L}_{\widehat{\Gamma}} & \widetilde{\mathcal{B}}_\gamma\mathbf{L}_{\widehat{\gamma}} \end{array} \right]}_{\mathcal{M}(\Gamma,\gamma)} \left[\begin{array}{c} \psi|_{\widehat{\Gamma}} \\ \psi|_{\widehat{\gamma}} \end{array} \right] = \left[\begin{array}{c} \mathbf{g} \\ \mathbf{0} \end{array} \right]. \tag{8}$$

The MFS consists in using the approximation justified by the density result

$$\mathbf{u}(x) = \mathbf{L}_{\Gamma\cup\gamma}\psi(x) \approx \sum_{i=1}^{n} \alpha_i \mathbf{\Phi}_{y_i}(x) =: \widetilde{\mathbf{u}}(x)$$

for some source points $y_1, \ldots, y_n \in \widehat{\Gamma} \cup \widehat{\gamma}$. We then compute the vectorial coefficients $\alpha_i = (\alpha_{i,1}, \alpha_{i,2})$ by solving the linear system

$$\left[\begin{array}{ccc} \mathbf{\Phi}_{y_1}(x_1) & \ldots & \mathbf{\Phi}_{y_n}(x_1) \\ \ldots & \ldots & \ldots \\ \mathbf{\Phi}_{y_1}(x_l) & \ldots & \mathbf{\Phi}_{y_n}(x_l) \\ \mathbf{\Phi}_{y_1}(x_{l+1}) & \ldots & \mathbf{\Phi}_{y_n}(x_{l+1}) \\ \ldots & \ldots & \ldots \\ \mathbf{\Phi}_{y_1}(x_m) & \ldots & \mathbf{\Phi}_{y_n}(x_m) \end{array} \right] \left[\begin{array}{c} \alpha_1 \\ \vdots \\ \alpha_n \end{array} \right] = \left[\begin{array}{c} \mathbf{g}(x_1) \\ \vdots \\ \mathbf{g}(x_l) \\ \mathbf{0} \\ \vdots \\ \mathbf{0} \end{array} \right] \tag{9}$$

on some collocation points $x_1, \ldots, x_l \in \Gamma$ and $x_{l+1}, \ldots, x_m \in \gamma$ $(l < m)$.

3.2 MFS version of the KKM

We now consider the inverse problem, ie., to obtain the shape of the boundary γ from the Cauchy data on Γ and will assume that $\widetilde{\mathcal{B}}_\Gamma$ is the Dirichlet boundary operator on Γ. The Kirsch-Kress Method (cf. [17]) was initially presented for acoustic scattering (twenty years ago), and the external boundary Γ was then replaced by the knowledge of the far field pattern.

The method consists in assuming that some knowledge on γ exists, such that we can prescribe an artificial boundary $\widehat{\gamma}$ inside γ and write the solution in terms of the inner boundary layer representation.

In the acoustic scattering problem the unknown density for the artificial inner boundary layer was recovered fitting its far field pattern. In the bounded domain we need to fit the Cauchy data and it is clear that the inner boundary will not be enough to adjust both Dirichlet and Neumann data. An extra external boundary layer must be considered.

At least two adaptations could be possible for the bounded domain:

(a) Use the boundary element method (BEM) formulation, and the extra boundary layer would be defined on the external accessible boundary Γ.

(b) Use the method of fundamental solutions (MFS) and define an external artificial boundary layer $\hat{\Gamma}$.

We will consider the second approach, and therefore it should be considered that we will use the MFS adaptation of the Kirsch-Kress Method (KKM).

Therefore the MFS version of the KKM method for the inverse bounded problem consists in two steps:

(i) **linear part:** solving the system of integral equations

$$\underbrace{\begin{bmatrix} \tau_\Gamma \mathbf{L}_{\widehat{\Gamma}} & \tau_\Gamma \mathbf{L}_{\widehat{\gamma}} \\ \tau_\Gamma^{\mathbf{n}} \mathbf{L}_{\widehat{\Gamma}} & \tau_\Gamma^{\mathbf{n}} \mathbf{L}_{\widehat{\gamma}} \end{bmatrix}}_{\mathcal{K}(\Gamma,\Gamma)} \begin{bmatrix} \phi|_{\widehat{\Gamma}} \\ \phi|_{\widehat{\gamma}} \end{bmatrix} = \begin{bmatrix} \mathbf{g} \\ \partial^*_{\lambda,\mu}\mathbf{u} \end{bmatrix}, \tag{10}$$

where τ_Γ, $\tau_\Gamma^{\mathbf{n}}$ are, respectively the trace and the normal trace on Γ.
Note that $\mathcal{K}(\Gamma,\Gamma)$ is $\mathcal{M}(\Gamma,\Gamma)$ with $\widetilde{\mathcal{B}}_\Gamma = \tau_\Gamma$ and $\widetilde{\mathcal{B}}_\gamma = \tau_\Gamma^{\mathbf{n}}$, when $\gamma = \Gamma$.

(ii) **nonlinear part:** the boundary γ will be given by the level set $\mathbf{u}^{-1}(\mathbf{0}) = \{x \in \Omega : \mathbf{u}(x) = \mathbf{0}\}$, for the Dirichlet problem (or computed iteratively, in an optimization scheme for a class of approximating shapes, for the Neumann or other boundary condition).

The linear part of the Kirsch-Kress Method to solve the Cauchy problem is therefore connected to the MFS since it may use the same boundary layers on $\widehat{\gamma}$ and on $\widehat{\Gamma}$ to give the solution of the direct problem from the Dirichlet boundary conditions on γ and Γ, and the reconstruction of the solution from the Dirichlet and Neumann data on Γ. In fact, the first line of the system (10) would be the same – known Dirichlet data. The same densities $\phi|_{\widehat{\Gamma}}$ and $\phi|_{\widehat{\gamma}}$ will verify both systems (8) and (10).

We now prove that a pair of Cauchy data can be retrieved using this MFS version of the KKM method.

Theorem 7. *The set*

$$\mathcal{S}_{\mathbf{n}} = span\left\{(\tau_\Gamma \mathbf{\Phi}_y, \tau_\Gamma^{\mathbf{n}} \mathbf{\Phi}_y) : y \in \widehat{\Gamma} \cup \widehat{\gamma}\right\}$$

is dense in $H^{1/2}(\Gamma)^2/\mathbb{R}^2 \times H^{-1/2}(\Gamma)^2$ *(or* $H^{1/2}(\Gamma)^3 \times H^{-1/2}(\Gamma)^3$ *in 3D).*

Proof. We follow the proof of Theorem 6. The adjoint of the matrix operator $\mathcal{K}(\Gamma,\Gamma)$ defined in (10) is given by

$$\mathcal{K}(\Gamma,\Gamma)^* = \begin{bmatrix} \tau_\Gamma \mathbf{L}_{\widehat{\Gamma}} & \tau_\Gamma \mathbf{L}_{\widehat{\gamma}} \\ \tau_\Gamma^{\mathbf{n}} \mathbf{L}_{\widehat{\Gamma}} & \tau_\Gamma^{\mathbf{n}} \mathbf{L}_{\widehat{\gamma}} \end{bmatrix}^* = \begin{bmatrix} \tau_{\widehat{\Gamma}} \mathbf{L}_\Gamma & \tau_{\widehat{\Gamma}} \mathbf{M}_\Gamma \\ \tau_{\widehat{\Gamma}} \mathbf{L}_{\widehat{\gamma}} & \tau_{\widehat{\gamma}} \mathbf{M}_\Gamma \end{bmatrix}.$$

In the 2D case, again the space $\mathcal{H}_{\mathbf{I}}(\Gamma)$ is identified to $H^{1/2}(\Gamma)^2/\mathbb{R}^2$ (taking the representative $\phi - \frac{1}{|\Gamma|}\int_\Gamma \phi$).

Let $\phi \in \mathcal{H}_{\mathbf{I}}(\Gamma), \psi \in H^{-1/2}(\Gamma)^2$ (2D case) or $\phi \in H^{1/2}(\Gamma)^3, \psi \in H^{-1/2}(\Gamma)^3$ (3D case) and define the function

$$\mathbf{u}(y) = (\mathbf{L}_\Gamma \phi)(y) + (\mathbf{M}_\Gamma \psi)(y)$$

a combination of single and double layer potentials defined on Γ. Following the same arguments, as in Theorem 6, we prove that if $\mathbf{u} = \mathbf{0}$ on $\hat{\Gamma} \cup \hat{\gamma}$ then by analytic continuation of the unique null solution of the interior and exterior problems (now $\mathbf{a}_{\tilde{\mathbf{Z}}} = \frac{\lambda+3\mu}{4\pi\mu(\lambda+2\mu)}\int_\Gamma \phi(x) dS_x = \mathbf{0}$, because $\phi \in \mathcal{H}_{\mathbf{I}}(\Gamma)$), we obtain $\mathbf{u} = \mathbf{0}$ in $\mathbb{R}^d \setminus \Gamma$. Then $\phi = [\partial^*_{\lambda,\mu}\mathbf{u}]_\Gamma = \mathbf{0}$ and $\psi = -[\mathbf{u}]_\Gamma = \mathbf{0}$. and the result follows. □

4 Numerical Simulations

In this section we consider three numerical simulations of the MFS - Kirsch-Kress Method applied to the recovery of a single inclusion. The accessible part of the boundary, Γ, is a centered circle with radius $r = 3.5$ and the boundary of the inclusion is given by the parametrization

$$\gamma_i(t) = \mathbf{c}_i + j_i(t)(\cos t, \sin t),\ 0 \le t \le 2\pi$$

with $\mathbf{c}_1 = (-1, 1)$, $j_1(t) = 1.1 + 1.6\cos^2(t/2)\sin(t/2)$, $\mathbf{c}_2 = (1, -0.3)$, $j_2(t) = 1.2 + 0.2\cos^2(2t)$, $\mathbf{c}_3 = (0, 0)$ and $j_3(t) = 1.3 - 0.3\cos(4t)$ (see Fig. 2). The Lamé constants are $\lambda = \mu = 1$ and as input function we use

$$\mathbf{g}_i(\mathbf{x}) = \mathbf{x} - \mathbf{c}_i - \nabla\log(|\mathbf{x} - \mathbf{c}_i|)$$

(in particular, we are assuming that the center of the inclusion is known in the inverse problem).

- The numerical solution of the direct problem was computed using the MFS and considering as artificial boundary,

  $$\widehat{\gamma}_i = \partial B(0, 4.2) \cup \gamma_i^{\#},$$

  with $\gamma_i^{\#}(t) = \mathbf{c}_i + 0.9 j_i(t)(\cos t, \sin t)$. We used 400 collocation and source points distributed uniformly on the boundary and artificial boundary and obtained good results (see Fig.3 for the plots of the absolute error of the first component on Γ and the second component on γ_3).

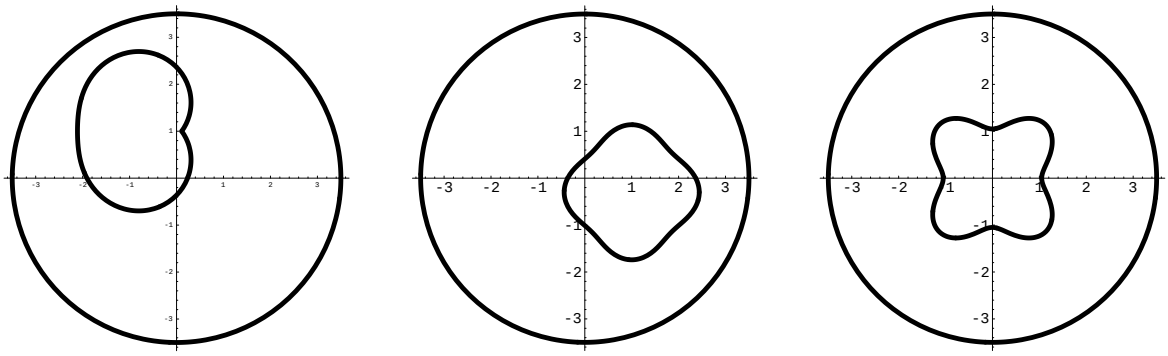

Figure 2: Geometry of the domains. Left- first test, middle- second test and right- third test.

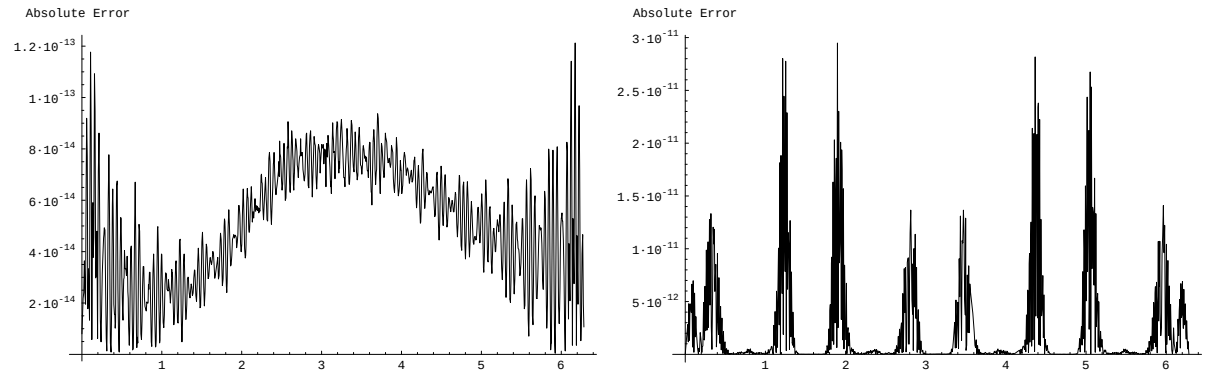

Figure 3: Absolute error on the boundary (third simulation): On the left–first coordinate on Γ, on the right– second coordinate on γ.

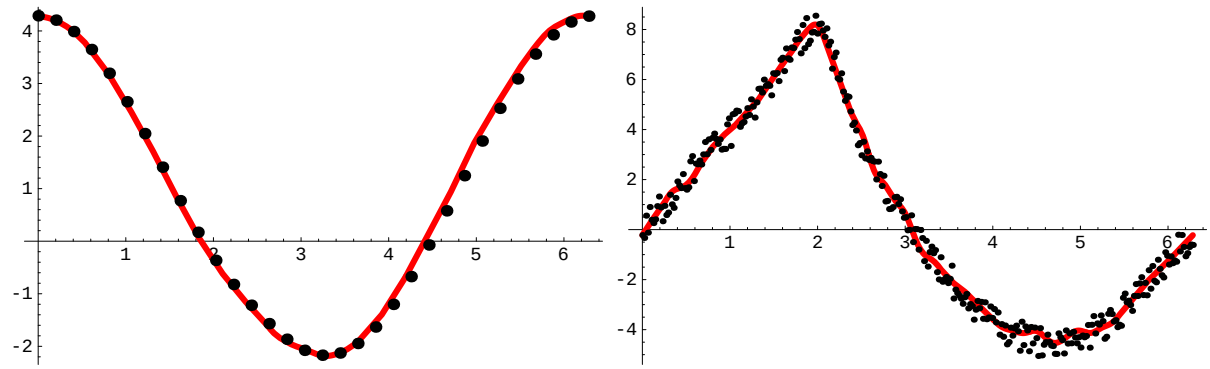

Figure 4: Comparison between the noisy Cauchy data on Γ and the computed data on the inverse problem (first simulation). On the left– first coordinate of the solution, on the right– second coordinate of the traction vector. Dots– data from the direct problem, thick red line– inverse problem. Noise level: 8 %.

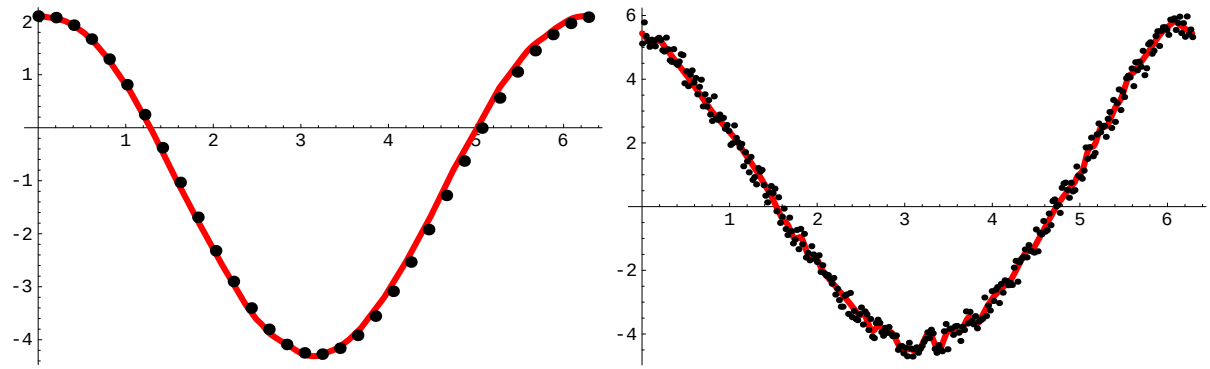

Figure 5: The same as in Fig. 4, for the second simulation. On the right picture we considered the first coordinate of the traction vector.

- For the inverse problem, we used $\partial B(0, 4.0) \cup \partial B(c_i, 0.7)$ as artificial boundary and solved the system of linear equations arising from the discretization of (10) in a least squares sense, using 300 source and 300 collocation points. To retrieve the curve, we performed a search along the segment joining radial points on Γ and on the internal artificial boundary and choose the point with minimum distance to the origin. Repeating this procedure for several points on Γ we obtain the approximation of γ.

For exact data, we retrieved the correct shape of the inclusion (first and second simulations). We present the numerical simulations for measured data affected by random (maximum norm) noise, i.e. the input vector is

$$[\partial^*_{\lambda,\mu}\mathbf{u}]^{noise}_k = [\partial^*_{\lambda,\mu}\mathbf{u}]_k + \varepsilon_k ||\partial^*_{\lambda,\mu}\mathbf{u}||_\infty$$

with random values ε_k such that $|\varepsilon_k| \leq \rho < 1$. A Tikhonov regularization procedure was implemented to solve the systems with an L-curve analysis to choose the regularization parameter. Figs. 4 and 5 shows the comparison between the given (noiseless) Cauchy data on Γ and the computed data on the inverse problem (introducing 8 % of random noise in the measured data) for simulations 1 and 2, respectively. For the first simulation, we present in Fig. 6 the results of the reconstructions with 3% and 8% of random noise.

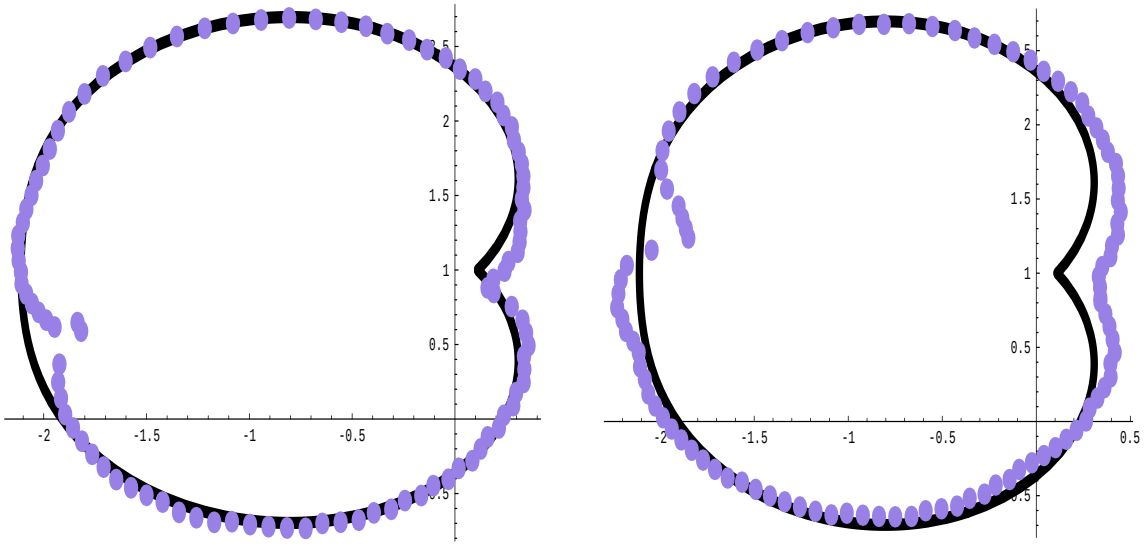

Figure 6: Reconstruction of the shape with 3 % (left) and 8 % (right) of noise. Full line- Shape of the inclusion; Dotted line- Reconstructed curve.

In the second simulation we present the effect of changing the center of the internal artificial curve in the reconstruction of the shape. Here, we tested for the artificial boundary $\partial B(c_2, 0.7)$ and $\partial B((1.3, -0.4), 0.7)$ (see Fig. 7) with 8 % of noise. The result obtained with the second choice of center is slightly better (and the corresponding system of equations is better conditioned) than the centered case.

The third simulation is presented using exact data. For this geometry the results are not so good even when tested with a non convex artificial internal domain (Fig. 8), yet the Cauchy data on Γ is well approximated (Fig. 9). In Fig.10 we present the absolute difference between the MFS solution of the direct problem and the inverse problem solution, which shows the instabilities that led to the problems observed in the reconstructions. In fact, the distance between the collocation and (inner) source points is bigger in the inverse problem and we observe a faster decay of the inverse problem matrix eigenvalues

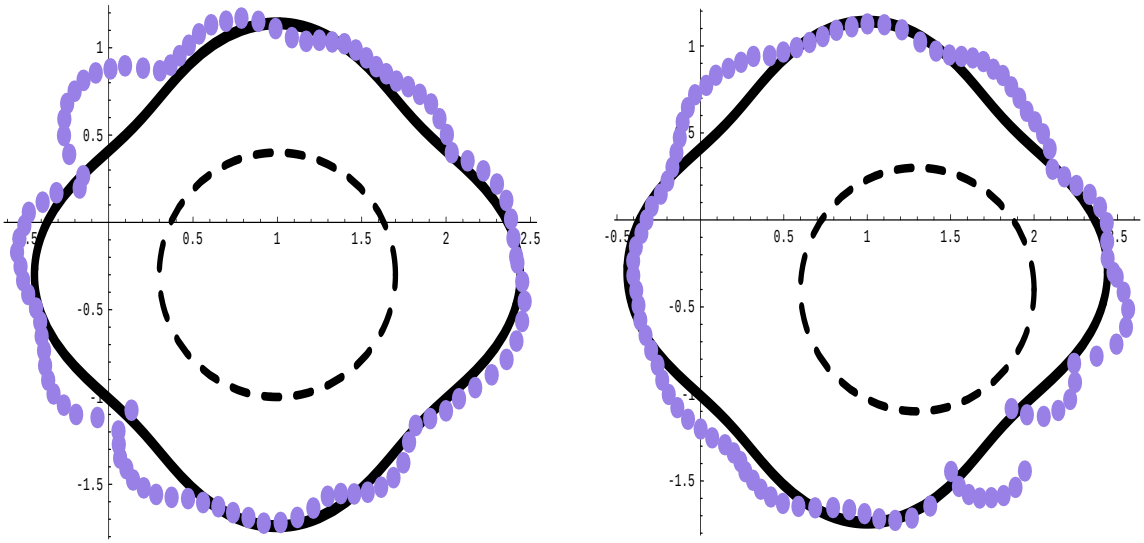

Figure 7: Reconstruction of the shape with internal circle (dashed line) centered with the inclusion (left) and on $(1.3, -0.4)$ (right). Noise level: 8 %

than in the direct problem (see Fig. 11). Recall that for the direct problem the artificial boundary is close to the boundary of Ω_c leading to a better conditioned system of equations whereas in the inverse problem only the outer part of the boundary is being considered and the internal part of the artificial boundary must be inside the inclusion.

5 Conclusions

In this work we discussed the question of the identification of inclusions/cavities in an elastic body, using a single boundary measurement. We proved the adequacy of the MFS to solve not only the direct problem, but also to solve the inverse (Cauchy) problem with a MFS version of the Kirsch-Kress Method. We proposed a fast procedure to reconstruct the shape of the inclusion and test it for several examples. In general, we were able to retrieve the localization and dimension of the inclusion and in some cases (mainly convex inclusions) a good reconstruction of the shape, for data affected by random (norm) noise.

Acknowledgments

Authors acknowledge the support of Fundação para a Ciência e Tecnologia (FCT), through projects POCI MAT/61792/2004, MAT/60863/2004 and ECM/58940/2004. N. Martins is also partially supported by FCT through the scholarship SFRH/BD/27914/2006.

References

[1] G. Alessandrini, A. Morassi, E. Rosset, *Detecting an inclusion in an elastic body by boundary measurements*, SIAM Review **46**, No. 3, 477–498, 2004.

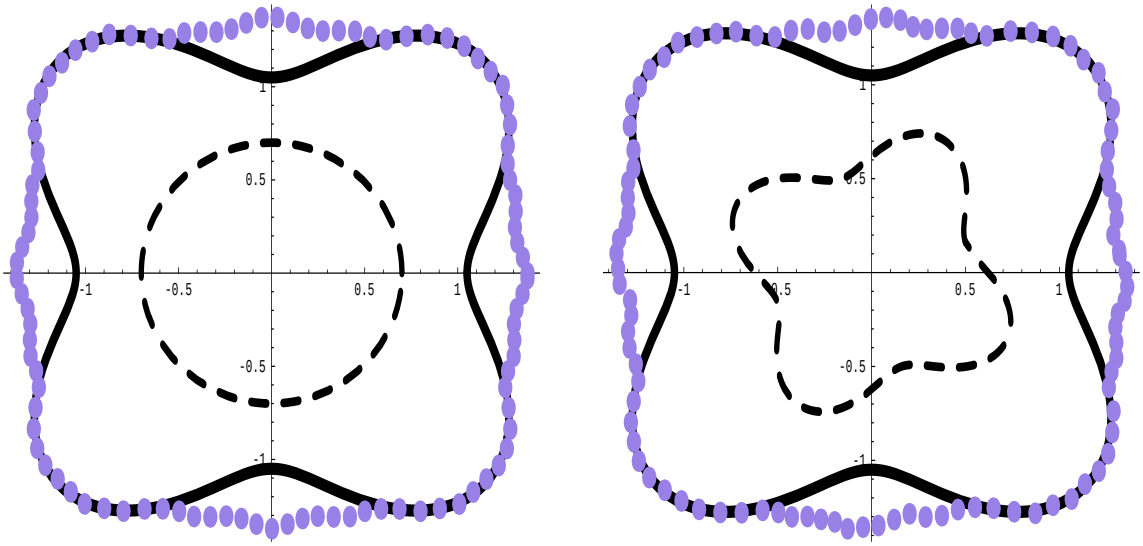

Figure 8: Reconstruction using different internal curves (exact data).

[2] C. J. S. Alves and H. Ammari, *Boundary integral formulae for the reconstruction of imperfections of small diameter in an elastic medium*, SIAM J. Appl. Math, **62**, 94–106, 2001.

[3] C. J. S. Alves and C. S. Chen, *A new method of fundamental solutions applied to nonhomogeneous elliptic problems*, Adv. Comp. Math., **23**, 125–142, 2005.

[4] H. Ammari, H. Kang, G. Nakamura and K. Kazumi, *Complete asymptotic expansions of solutions of the system of elastostatics in the presence of an inclusion of small diameter and detection of an inclusion*, Journal of Elasticity, **67**(2), 97–129, 2002.

[5] E. Argyropoulos and K. Kiriaki, *Modified Green's function technique for disjoint bodies in two-dimensional linear elasticity*, Bull. Greek Math. Soc., **47**, 137–151, 2003.

[6] K. Baganas, A. Charalambopoulos and G. D. Manolis, *Detection of spherical inclusions in a bounded, elastic cylindrical domain*, Wave Motion, **41**(1), 13–28, 2005.

[7] A. Bogomolny, *Fundamental solutions method for elliptic boundary value problems*, Siam, J. Numer. Anal., **22**, 644–669, 1985.

[8] M. Bonnet and A. Constantinescu, *Inverse problems in elasticity*, Inverse Problems, **21**, R1–R50, 2005.

[9] K. Bryan and L. Caudill, *An Inverse problem in thermal imaging*, SIAM J. Appl. Math., **56**, 715–735, 1996.

[10] F. Cakoni and R. Kress, Integral equations for inverse problems in corrosion detection from partial Cauchy data, Inverse Problems an Imaging, **1**(2), 229-245, 2007

[11] G. Chen and J. Zou , *Boundary Element Methods*, Academic Press, London, 1992.

[12] D. Colton and R. Kress , *Inverse Acoustic and Electromagnetic Scattering Theory*, 2. ed., Applied Mathematical Sciences, 93, Springer, 1998.

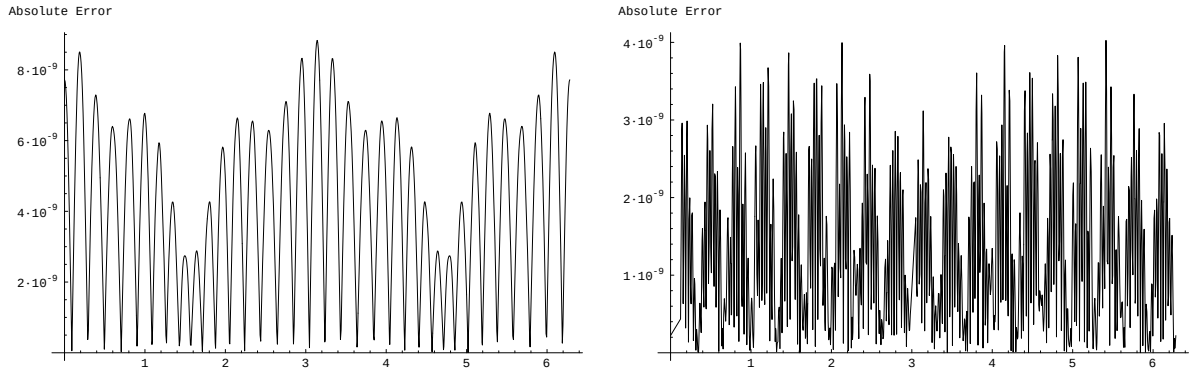

Figure 9: Error on Γ for the computed solution of the Cauchy problem: left- first coordinate; right- second coordinate of the traction vector.

[13] L. C. Evans, *Partial Differential Equations*, Springer-Verlag, New York, 1991.

[14] G. Fairweather and A. Karageorghis, *The method of fundamental solutions for elliptic boundary value problems*, Adv. Comput. Math., **9**, 69–95, 1998.

[15] D. Fasino and G. Inglese, *Discrete methods in the study of an inverse problem for Laplace's equation*, IMA Journal of Numerical Analysis, **19**, 105–118, 1999.

[16] G. Inglese, *An inverse problem in corrosion detection*, Inverse Problems, **13**, 977–994, 1997.

[17] A. Kirsch and R. Kress, *On an integral equation of the first kind in inverse acoustic scattering*, Inverse Problems, ISNM **77**, 93–102, 1986.

[18] V. D. Kupradze and M. A. Aleksidze, *The method of functional equations for the aproximate solution of certain boundary value problems*, Zh. vych. mat., **4**, 683–715, 1964.

[19] K. Madsen, H.B. Nielsen and O. Tingleff, *Methods for non-linear Least Squares Problems*, IMM, 60 pages, Denmark, 2004.

[20] L. Marin, *A meshless method for solving the Cauchy problem in three-dimensional elastostatics*, Comput. Math. Appl. **50**, 73-92, 2005.

[21] A. Morassi and E. Rosset, *Detecting rigid inclusions or cavities, in an elastic body*, Journal of elasticity, **73**, 101–126, 2003.

[22] N. I. Muskhelishvili, *Some basic problems of mathematical theory of elasticity*, North International Publishing, The Netherlands, 1975.

[23] G. Nakamura and G. Uhlmann, *Identification of Lamé parameters by boundary measurements*, American Journal of Mathematics, **115**, 1161–1187, 1993.

[24] R. Potthast and J. Schulz, *From the Kirsch-Kress potential method via the range test to the singular sources method*, Journal of Physics: Conference Series, **12**, 116–127, 2005.

[25] V. S. Vladimirov, *Equations of mathematical physics*. MIR, Moscow, 1984.

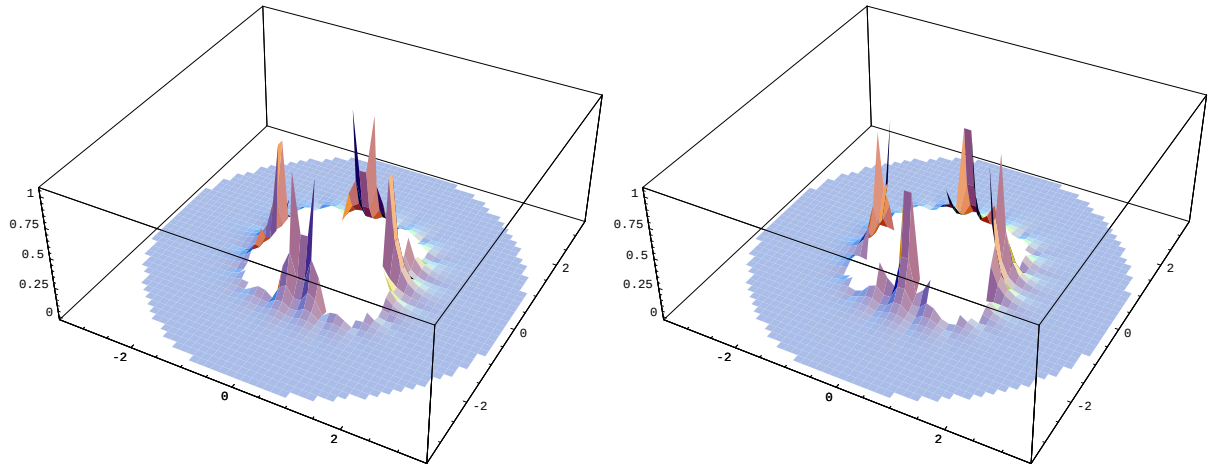

Figure 10: Absolute difference between the solution of the direct problem and the inverse problem: Left- first coordinate; Right- second coordinate.

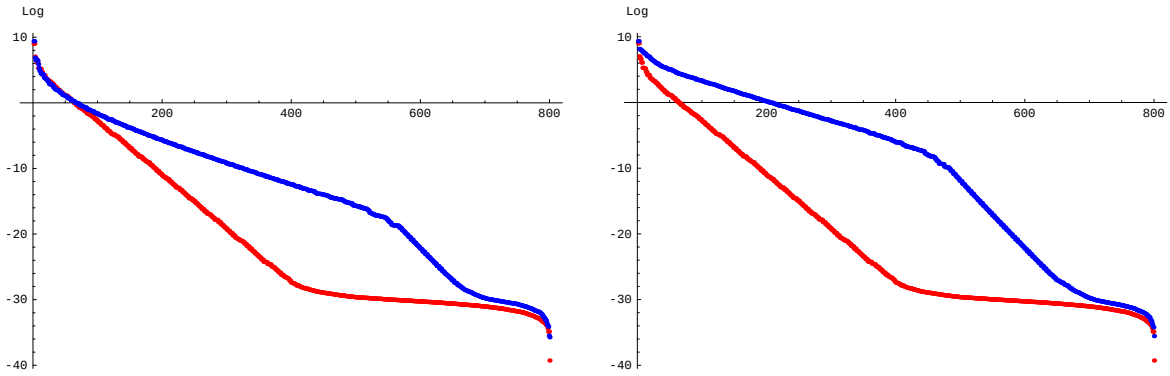

Figure 11: Eigenvalues of the system arising from the discretization of the problems: Left- Inclusion reconstruction (homogeneous Dirichlet condition on γ); Right- cavity reconstruction (homogeneous Neumann condition on γ). Blue (top) curve- direct problem using MFS; Red (bottom) curve- inverse problem using the Kirsch Kress method.